Journal of Anatomy

J. Anat. (2020) **236**, pp317–324 doi: 10.1111/joa.13096

Ift88 is involved in mandibular development

Atsushi Kitamura,[1,2] Maiko Kawasaki,[1,3] Katsushige Kawasaki,[1,3,4] Fumiya Meguro,[1] Akane Yamada,[1,2] Takahiro Nagai,[1,2] Yasumitsu Kodama,[2] Supaluk Trakanant,[1,6] Paul T. Sharpe,[3] Takeyasu Maeda,[1,4,5] Ritsuo Takagi[2] and Atsushi Ohazama[1,3]

[1]*Division of Oral Anatomy, Niigata University Graduate School of Medical and Dental Sciences, Niigata, Japan*
[2]*Division of Oral and Maxillofacial Surgery, Niigata University Graduate School of Medical and Dental Sciences, Niigata, Japan*
[3]*Centre for Craniofacial Development and Regeneration, Dental Institute, Guy's Hospital, King's College London, London, UK*
[4]*Research Center for Advanced Oral Science, Niigata University Graduate School of Medical and Dental Sciences, Niigata, Japan*
[5]*Faculty of Dental Medicine, University of Airlangga, Surabaya, Indonesia*
[6]*Division of Orthodontics, Niigata University Graduate School of Medical and Dental Sciences, Niigata, Japan*

Abstract

The mandible is a crucial organ in both clinical and biological fields due to the high frequency of congenital anomalies and the significant morphological changes during evolution. Primary cilia play a critical role in many biological processes, including the determination of left/right axis patterning, the regulation of signaling pathways, and the formation of bone and cartilage. Perturbations in the function of primary cilia are known to cause a wide spectrum of human diseases: the ciliopathies. Craniofacial dysmorphologies, including mandibular deformity, are often seen in patients with ciliopathies. Mandibular development is characterized by chondrogenesis and osteogenesis; however, the role of primary cilia in mandibular development is not fully understood. To address this question, we generated mice with mesenchymal deletions of the ciliary protein, *Ift88* (*Ift88*$^{fl/fl}$;*Wnt1Cre*). *Ift88*$^{fl/fl}$;*Wnt1Cre* mice showed ectopic mandibular bone formation, whereas *Ift88* mutant mandible was slightly shortened. Meckel's cartilage was modestly expanded in *Ift88*$^{fl/fl}$;*Wnt1Cre* mice. The downregulation of Hh signaling was found in most of the mesenchyme of *Ift88* mutant mandible. However, mice with a mesenchymal deletion of an essential molecule for Hh signaling activity, *Smo* (*Smo*$^{fl/fl}$;*Wnt1Cre*), showed only ectopic mandibular formation, whereas *Smo* mutant mandible was significantly shortened. *Ift88* is thus involved in chondrogenesis and osteogenesis during mandibular development, partially through regulating Sonic hedgehog (Shh) signaling.

Key words: Hedgehog signaling; Ift88; mandibular bone; Meckel's cartilage.

Introduction

Approximately one-third of all congenital defects include craniofacial anomalies. In particular, mandible anomalies, including micrognathia, have been shown to occur at high frequency. The mandible is also known to be a key factor in evolution due to the significant morphological changes that occurred during evolution. Therefore, understanding the molecular mechanisms regulating mandibular development is crucial for both biological and clinical fields.

The mandible shows unique developmental processes (Achilleos & Trainor, 2015; Parada & Chai, 2015; Terrazas et al. 2017). Mandibular development relies on chondrogenesis (Meckel's cartilage) and osteogenesis (mandibular bone). Meckel's cartilage is believed to act as a transient supportive tissue for mandibular bone formation during embryogenesis and disappears at late gestation and in early neonates. Meckel's cartilage initiates in the molar tooth region of the mandibular process and then extends in both directions along the anterior–posterior axis. The mandibular bone is first seen as condensed mesenchymal cells that proliferate and differentiate into osteogenic cells. The ossification of the mandibular bone mainly begins in the mesenchyme buccal and extends until Meckel's cartilage at the molar tooth region, and the developing mandibular bone subsequently surrounds Meckel's cartilage. However, in murine mandible, except in the incisor region, the bulk of the mandibular bone forms in the mesenchyme buccal to Meckel's cartilage, and only a thin portion of bone is formed in the mesenchyme lingual to Meckel's cartilage.

Correspondence
Atsushi Ohazama, Division of Oral Anatomy, Niigata University Graduate School of Medical and Dental Sciences, 2-5274 Gakkocho-dori, Chuo-ku, Niigata, 951-8514, Japan.
E: atsushiohazama@dent.niigata-u.ac.jp

Accepted for publication *4 September 2019*
Article published online *28 October 2019*

Primary cilia are immotile organelles on the surface of almost all mammalian cells. Cilia play important roles in many biological processes, including determination of left/right axis patterning and regulation of signaling pathways (Bisgrove & Yost, 2006; Zaghloul & Brugmann, 2011). Hedgehog (Hh) signaling is activated within primary cilia. Primary cilium comprises a membrane-bound cylinder surrounding nine doublet microtubules that extend from a basal body. Cilia are assembled and maintained by an intraflagellar transport (IFT) system, in which multiple protein complexes move bidirectionally along the axoneme by the coordinated action of IFT motor proteins. IFT is a highly conserved system in all ciliated eukaryotic cells, and perturbations in the function of primary cilia are implicated in a wide spectrum of human diseases: the ciliopathies (Bisgrove & Yost, 2006). Mandibular abnormalities are observed in many ciliopathy patients. Primary cilia are reportedly involved in chondrogenesis and osteogenesis (Yuan & Yang, 2016); however, their role in mandibular development is not fully understood (Kolpakova-Hart et al. 2007; Gray et al. 2009; Brugmann et al. 2010; Zhang et al. 2011, 2011; Adel Al-Lami et al. 2016; Cela et al. 2018; Kitami et al. 2019).

Ift88 encodes a protein that is required for IFT (Murcia et al. 2000). By analyzing mice with tissue-specific conditional deletions of *Ift88*, we discovered that *Ift88* regulates mandibular development by controlling chondrogenesis and osteogenesis.

Materials and methods

Production and analysis of transgenic mice

P53$^{-/-}$, *Ift88*$^{fl/fl}$, *Wnt1Cre*, *R26SmoM2*, and *K14Cre* mice were produced as described previously (Danielian et al. 1998; Jeong et al. 2004; Narai et al. 2006; Yi et al. 2006; Haycraft et al. 2007). Embryonic day 0 (E0) was taken to be midnight prior to finding a vaginal plug.

In situ hybridization

In situ hybridization was carried out as described previously (Ohazama et al. 2008).

Skeletal preparation

To analyze the skeleton, pups were stained with Alcian Blue for nonmineralized cartilage and Alizarin Red for bone. Briefly, mice were fixed in 100% ethanol and then stained for 5 days in 0.1% Alizarin Red S (in 95% ethanol), 0.3% Alcian Blue (in 70% ethanol), 100% acetic acid, and ethanol, followed by alkaline hydrolysis and glycerol clearing.

3D reconstruction of Meckel's cartilage

The 3D reconstructions of Meckel's cartilage were made from serial sections as described previously (Kawasaki et al. 2014) using the Amira software package (Template Graphics Software).

Cell proliferation

For detection of cell proliferation, pregnant females were injected intraperitoneally with BrdU (Roche) labeling reagent (45 mg g^{-1} body weight) at E12.5. One hour after injection, embryos were fixed in 4% paraformaldehyde (PFA) fixative and embedded in paraffin wax, from which sections were cut. Immunodetection of BrdU was performed using the BrdU labeling and detection kit (Roche) according to the manufacturer's instructions.

Results

Mandible phenotypes in *Ift88*$^{fl/fl}$*;Wnt1Cre* mice

Global mutations in *Ift88* have been shown to lead to early embryonic lethality (Murcia et al. 2000). Therefore, mice with tissue conditional mutations in *Ift88* were generated using the Cre–LoxP system. First, we generated mice with a mesenchymal loss of *Ift88* in neural crest-derived cells using *Wnt1Cre* (*Ift88*$^{fl/fl}$*;Wnt1Cre*). *Ift88*$^{fl/fl}$*;Wnt1Cre* mice died at birth and had no tongue (Tian et al. 2017). Skeletal preparation analysis showed that *Ift88* mutant mandibles were slightly shorter and thicker than those of wild-type mice along the anterior–posterior and left/right axis, respectively at E18.5 (Fig. 1A,B,D,E,G,H). In wild-type mice, developing mandibular bone extends along the anterior–posterior axis and, subsequently, the posterior end of the mandible starts to form three mandibular processes that are classified as secondary cartilage: condylar, coronoid, and angular. In wild-type mice, cartilage was observed only in the angular and condylar processes at birth (Fig. 1A,D,G,J). In *Ift88*$^{fl/fl}$*;Wnt1Cre* mice, extra cartilage formation was observed in the lingual side of the mandible at the posterior end of the mandible (Fig. 1E,K). This extra cartilage was isolated from other endogenous cartilage. Examination of the aboral side of *Ift88* mutant mandibles indicated that two mandibular bones were present, and the extra cartilage at the posterior end of the mandible was found to form in the lingual side of the mandibular bone (Fig. 1H, Supporting Information Fig. S1B). These two mandibular bones could not be observed in the anterior mandibles of *Ift88*$^{fl/fl}$*;Wnt1Cre* mice (Fig. 1H). The oral side of *Ift88* mutant mandibles did not show these two mandibular bones, except at the posterior end of the mandibles (Fig. S1D,F). The anterior mutant mandible was slightly enlarged along the left/right axis (Figs 1E,H and S1F). Examination of the buccal and lingual sides of the mandibles indicated that *Ift88* mutant mandibular bone was also enlarged along the oral–aboral axis and that the coronoid process was ablated in *Ift88*$^{fl/fl}$*;Wnt1Cre* mice (Fig. 1N,Q). Histological analysis revealed that mandibular bone oral, lingual, and buccal to Meckel's cartilage was enlarged in the anterior mandible of *Ift88*$^{fl/fl}$*;Wnt1Cre* mice (Fig. 2B). In the middle and posterior mandibles, enlarged mandibular bone lingual to Meckel's cartilage (lingual mandibular bone) and the mandibular bone

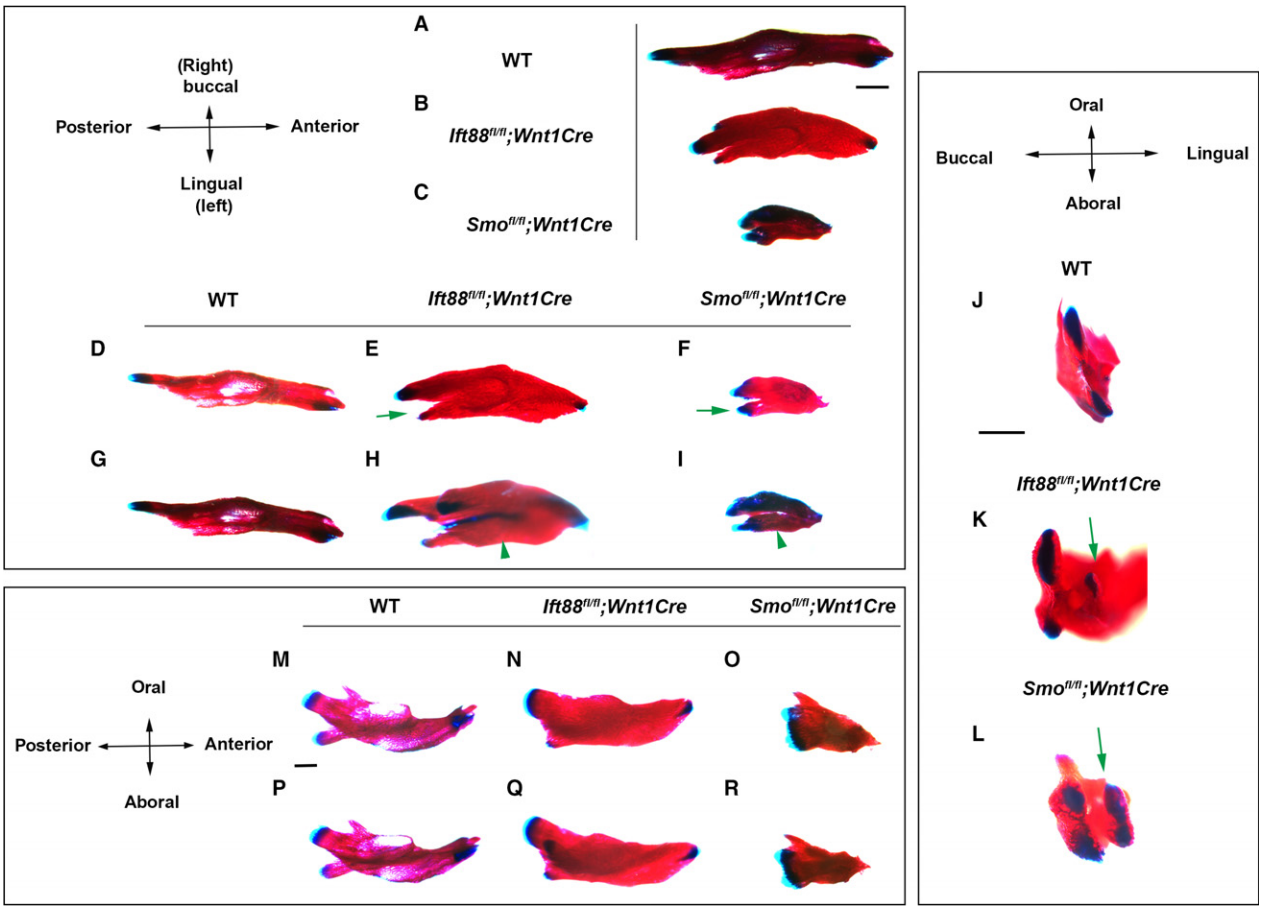

Fig. 1 Mandibular bone phenotypes in *Ift88*$^{fl/fl}$*;Wnt1Cre* and *Smo*$^{fl/fl}$*;Wnt1Cre* mice. Oral (A–F), aboral (G–I), buccal (M–O) and lingual (P–R) view of skeletal preparation of wild-type, *Ift88*$^{fl/fl}$*;Wnt1Cre* and *Smo*$^{fl/fl}$*;Wnt1Cre* mice at E18.5. (J–L) Proximal end of skeletal preparation of wild-type, *Ift88*$^{fl/fl}$*;Wnt1Cre* and *Smo*$^{fl/fl}$*;Wnt1Cre* mice at E18.5. Green arrows and arrowheads indicate extra cartilage formation and ectopic mandibular bone formation, respectively. Scale bars: 1 mm.

buccal to Meckel's cartilage (buccal mandibular bone) were observed in *Ift88*$^{fl/fl}$*;Wnt1Cre* mice (Fig. 2E, data not shown). There was a gap between the lingual and buccal mandibular bone at the aboral side of the mandible, but thin bone formation was observed between them at the oral side of the mandible (Fig. 2H). To examine Meckel's cartilage present between the lingual and buccal mandibular bone in *Ift88*$^{fl/fl}$*;Wnt1Cre* mice, in addition to the analysis of skeletal preparations using Alcian Blue, we performed a 3D reconstruction of Meckel's cartilage from histological specimens to obtain a more detailed picture of Meckel's cartilage. Both analyses showed that Meckel's cartilage was slightly shortened and thickened in *Ift88*$^{fl/fl}$*;Wnt1Cre* mice (Fig. 3B, data not shown). The enlargement of chondrocytes could not be detected in *Ift88*$^{fl/fl}$*;Wnt1Cre* mice (data not shown). These mandibular bone phenotypes were observed to be fully penetrant in *Ift88*$^{fl/fl}$*;Wnt1Cre* mice. To determine whether *Ift88* in epithelium is also involved in mandibular development, we next generated mice with epithelial conditional *Ift88* mutations using *Keratin(K)14Cre* (*Ift88*$^{fl/fl}$*;K14Cre*). We found that *Ift88*$^{fl/fl}$*;K14Cre* mice exhibited no obvious abnormalities in mandibular development (data not shown).

Initiation of abnormal mandible formation in *Ift88*$^{fl/fl}$*;Wnt1Cre* mice

Ectopic condensed mesenchyme and cell proliferation examined by BrdU were observed in the region lingual to Meckel's cartilage in *Ift88*$^{fl/fl}$*;Wnt1Cre* mice (Fig. S2B,D). To further identify the region where abnormal mandibular development initiates in *Ift88*$^{fl/fl}$*;Wnt1Cre* mice, we analyzed the osteoblast differentiation marker, *Runx2*, at early stages of mandibular development. At E12.5, *Runx2* was expressed in mesenchyme buccal to Meckel's cartilage in wild-type mice, which was slightly expanded in *Ift88*$^{fl/fl}$*;Wnt1Cr* mice (Fig. 4A,B,D,E). *Ift88*$^{fl/fl}$*;Wnt1Cre* mice also showed ectopic *Runx2* expression in mesenchyme lingual to Meckel's cartilage, which was observed as an oblique expression domain in *Ift88* mutant mandibles from the

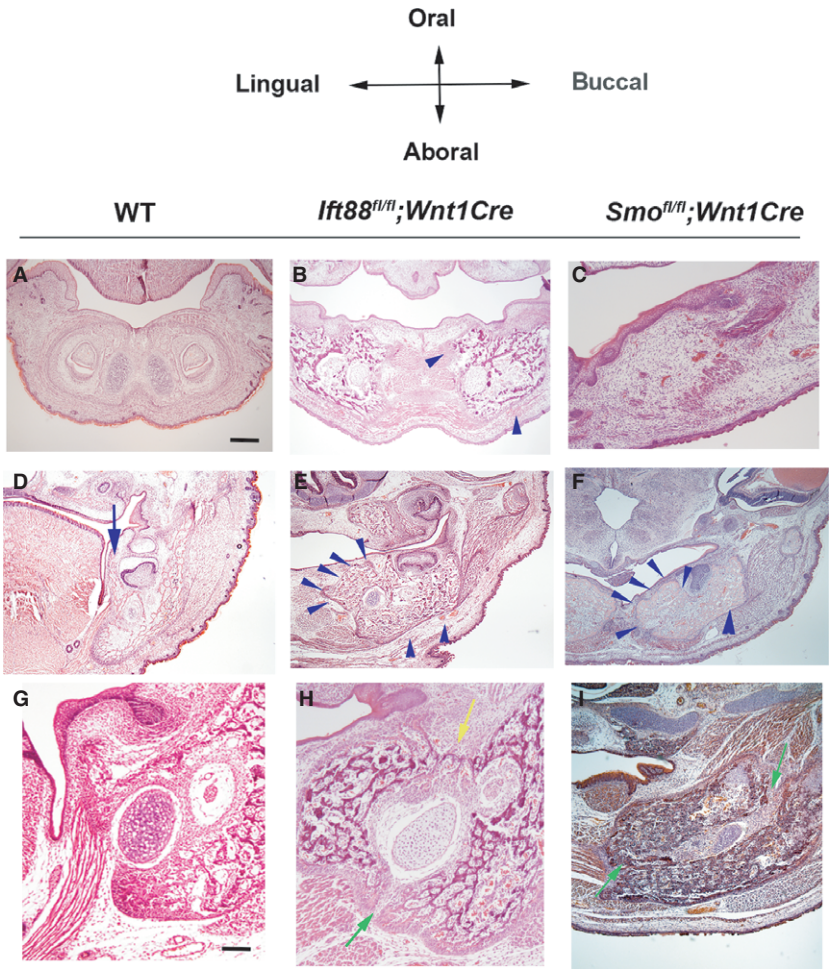

Fig. 2 Histological mandibular bone phenotypes in *Ift88*$^{fl/fl}$*;Wnt1Cre* and *Smo*$^{fl/fl}$*;Wnt1Cre* mice. Frontal sections show the developing mandibular bone in wild-type, *Ift88*$^{fl/fl}$*;Wnt1Cre* and *Smo*$^{fl/fl}$*;Wnt1Cre* mice at E18.5. Blue arrow and arrowheads indicate wild-type endogenous lingual mandibular bone and mutant excess mandibular bone, respectively. Green arrow indicates the gap between lingual and buccal bone. Yellow arrow indicate the thin bone between lingual and buccal bone. Scale bars: 500 μm (A–F), 250 μm (G–I).

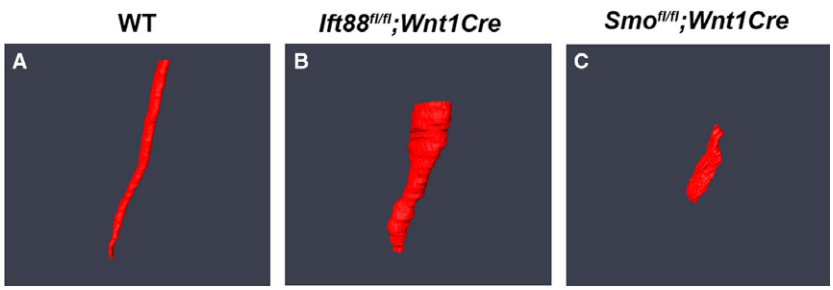

Fig. 3 Meckel's cartilage in *Ift88*$^{fl/fl}$*;Wnt1Cre* and *Smo*$^{fl/fl}$*;Wnt1Cre* mice. 3D reconstruction of Meckel's cartilage of wild-type, *Ift88*$^{fl/fl}$*;Wnt1Cre* and *Smo*$^{fl/fl}$*;Wnt1Cre* mice at E14.5.

anterior mandible to the lingual end of the posterior mandible (Fig. 4B,E).

Molecular changes in the developing mandible of *Ift88*$^{fl/fl}$*;Wnt1Cre* mice

To identify candidate molecules related to the mandibular phenotypes in *Ift88*$^{fl/fl}$*;Wnt1Cre* mice, we performed *in situ* hybridization and immunohistochemistry analyses in the region where extra bone formation initiated at E11.5 and E12.5. It has been shown that Fgf, Wnt, Tgfβ, and Bmp signaling pathways are involved in craniofacial development, including mandibular development (Brugmann et al. 2007; Mina et al. 2007; Oka et al. 2008; Komatsu et al. 2013). No *Ift88*$^{fl/fl}$*;Wnt1Cre* mice exhibited any significant differences in the expression of marker molecules for these pathways in

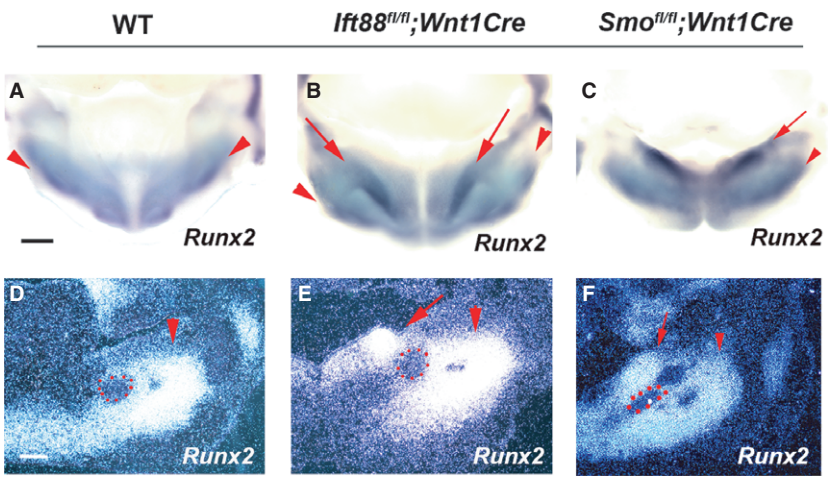

Fig. 4 Initiation of mandibular bone formation. (A–C) Oral view of whole mount showing *Runx2* expression. (D–F) Frontal sections showing *in situ* hybridization of *Runx2*. Arrowheads and arrows indicate endogenous and ectopic mandibular bone region, respectively. Scale bars: 500 μm.

developing mandibles (data not shown). Hh signaling is activated within primary cilia and is involved in craniofacial development (Jeong et al. 2004; Bisgrove & Yost, 2006; Zaghloul & Brugmann, 2011; Kurosaka et al. 2014). Therefore, expression of *Ptch1* and *Gli1* (direct targets of Hh signaling) was examined in developing mandibular. In wild-type mandibular mesenchyme, *Ptch1* and *Gli1* expression was broadly observed at E11.5 (Fig. 5A,B). At E12.5, *Ptch1* and *Gli1* expression was also found in entire mesenchyme of the anterior mandible, but became restricted in the middle and posterior mandible (Fig. 5C,E,G,I). In the middle and posterior mandibles, both *Ptch1* and *Gli1* showed expression in the endogenous bone region at E12.5. *Ptch1* was also expressed in mesenchyme lingual to Meckel's cartilage, whereas *Gli1* expression could not be detected in the region (Fig. 5E,I). *Ptch1* and *Gli1* expression was significantly downregulated in most of the mesenchyme from the anterior to posterior mandible, including the region corresponding to endogenous and ectopic mandibular bone formation in *Ift88*$^{fl/fl}$*;Wnt1Cre* mice (Fig. 5D,F,H,J). Unlike in mesenchyme, both *Ptch1* and *Gli1* expression was found to be increased in *Ift88* mutant mandibular epithelium, indicating that Hh signaling was overactivated in mandibular epithelium of *Ift88*$^{fl/fl}$*;Wnt1Cre* mice. The jaw is known to develop via an epithelial–mesenchymal interaction (Billmyre & Klingensmith, 2015; Li et al. 2017). It has been shown that mice with overexpression of *Shh* in the epithelium (*K14-Shh*) show enlarged mandibles, suggesting the possibility that the overactivation of Hh signaling in mandibular epithelium results in extra mandibular bone formation (Cobourne et al. 2009). However, Hh signaling is likely overactivated both in epithelium and mesenchyme in *K14-Shh* mice, since overexpression of Shh protein can bind to receptors expressing both in epithelium and mesenchyme. Hh signaling was overactivated only in mandibular epithelium of *Ift88*$^{fl/fl}$*;Wnt1Cre* mice. To address this question, we generated mice with overactive Hh signaling only in the epithelium using *R26SmoM2*, since Hh signaling is overactivated only in epithelium, when *R26SmoM2* mice are crossed with *K14Cre* driver mice (*R26SmoM2;K14Cre*). *R26SmoM2;K14Cre* mice exhibited no extra mandibular bone formation, suggesting that the upregulated Hh signaling observed in *Ift88* mutant mandibular epithelium is not the cause of extra mandibular bone formation (Supporting Information Fig. S3).

Hh signaling in Ift88 mutant mandibles

It has been shown that mice with a mesenchymal conditional mutation in *Smo* (an essential molecule in Hh signaling) generated using *Wnt1Cre* mice (*Smo*$^{fl/fl}$*;Wnt1Cre*) exhibit abnormal mandibular formation (Jeong et al. 2004; Xu et al. 2019). To investigate whether abnormal mandibular bone formation in *Ift88*$^{fl/fll}$*;Wnt1Cre* mice was the result of the downregulation of the Hh signaling pathway in mesenchyme, we compared the mandibular phenotypes in *Ift88*$^{fl/fll}$*;Wnt1Cre* and *Smo*$^{fl/fl}$*;Wnt1Cre* mice. *Smo*$^{fl/fl}$*;Wnt1Cre* mice have been shown to exhibit significantly smaller lower jaws than wild-type mice (Fig. 1C; Jeong et al. 2004; Xu et al. 2019). In common with *Ift88*$^{fl/fll}$*;Wnt1Cre* mice, *Smo*$^{fl/fl}$*;Wnt1Cre* mice exhibited extra cartilage at the posterior end of the mandible, which was separated from endogenous cartilage in the angular and condylar processes (Fig. 1F,L). The extra cartilage in the *Smo*$^{fl/fl}$*;Wnt1Cre* mice was bigger than that in the *Ift88*$^{fl/fll}$*;Wnt1Cre* mice. Contrary to *Ift88*$^{fl/fll}$*;Wnt1Cre* mice, the coronoid process was also present in *Smo*$^{fl/fl}$*;Wnt1Cre* mice (Fig. 1O,R). In common with *Ift88*$^{fl/fll}$*;Wnt1Cre* mice, the aboral side of the *Smo* mutant mandibles showed two mandibular bones (Fig. 1I). However, unlike in *Ift88*$^{fl/fll}$*;Wnt1Cre* mice, these two mandibular bones were observed along the entire mandible of *Smo*$^{fl/fl}$*;Wnt1Cre* mice. Through histological analysis, no bone

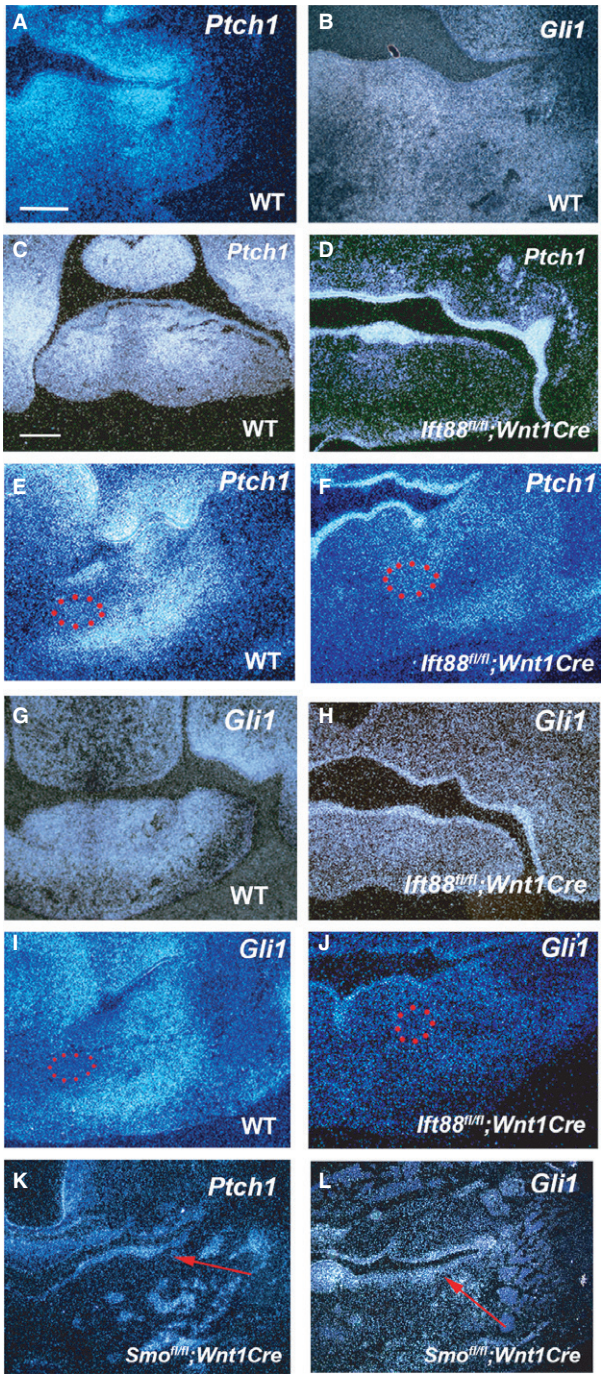

Fig. 5 Shh signaling in mandibles in *Ift88*$^{fl/fl}$*;Wnt1Cre* and *Smo*$^{fl/fl}$*; Wnt1Cre* mice. Frontal sections show *in situ* hybridization of *Ptch1* (A, C–F,K) and *Gli1* (B,G–J,L) in the anterior (C,D,G,H) and middle (molar) region (A,B,E,F,I–L) of wild-type (A,B,C,E,G,I), *Ift88*$^{fl/fl}$*;Wnt1Cre* (D,F,H, J) and *Smo*$^{fl/fl}$*;Wnt1Cre* (K, L) mice at E11.5 (A, B) and E12.5 (C–L). Meckel's cartilage is outlined by red dots. Scale bars: 250 μm.

formation was observed in the anterior mandible of *Smo*$^{fl/fl}$*; Wnt1Cre* mice (Fig. 2C). Like *Ift88*$^{fl/fll}$*;Wnt1Cre* mice, enlarged lingual and buccal mandibular bone was observed in the middle and posterior part of *Smo* mutant mandibles (Fig. 2F, data not shown). In *Smo*$^{fl/fl}$*;Wnt1Cre* mice, Meckel's cartilage was also present between the lingual and buccal mandibular bone and was significantly shortened and slightly thickened (Fig. 3C; Jeong et al. 2004; Billmyre & Klingensmith, 2015; Xu et al. 2019). There was a gap between the lingual and buccal bone at both the oral and aboral side of mandible in the *Smo* mutant mandible (Fig. 2I). *Runx2* expression was slightly expanded in the region buccal to Meckel's cartilage, whereas ectopic *Runx2* expression was observed in mesenchyme lingual to Meckel's cartilage in *Smo*$^{fl/fl}$*;Wnt1Cre* mice (Fig. 4C,F). Unlike in *Ift88*$^{fl/fll}$*;Wnt1Cre* mice, the ectopic *Runx2* expression domain was retained at the lingual end of *Smo*$^{fl/fl}$*;Wnt1Cre* mutant mandibles. Interestingly, upregulation of *Ptch1* and *Gli1* expression were also observed in the mandibular epithelium of *Smo*$^{fl/fl}$*;Wnt1Cre* mice (Fig. 5K,L).

The relationship between ectopic bone formation in the palatal shelf and the mandible

We previously reported that ectopic bone is formed in the maxillary processes of *Ift88*$^{fl/fl}$*;Wnt1Cre* mice as a result of abnormal apoptosis. The ectopic bone disappears when the apoptosis regulating molecule *p53* is deleted from *Ift88*$^{fl/fl}$*; Wnt1Cre* mice (*Ift88*$^{fl/fl}$*;Wnt1Cre;p53*$^{-/-}$; Watanabe et al. 2019). However, in the present study, no abnormal apoptotic activity was detected in *Ift88* mutant mandible, and the abnormal mandibular bone showed no changes in *Ift88*$^{fl/fl}$*;Wnt1Cre;p53*$^{-/-}$ mice (Supporting Information Fig. S4, data not shown).

Discussion

In wild-type mice, only thin bone formation was observed in the region lingual to Meckel's cartilage in the middle and posterior mandible. *Runx2* was not obviously expressed in that region at the early stage of mandibular development. In *Ift88*$^{fl/fll}$*;Wnt1Cre* mice, *Runx2* was ectopically expressed in the region and the subsequent lingual mandibular bone was significantly enlarged. Extra cartilage formation was also observed at the posterior end of the *Ift88* mutant mandible along with the angular and condylar processes, which was formed in the enlarged lingual mandibular bone. It has been shown that cartilage in the angular and condylar processes is derived from the periosteum of the ossifying mandible in wild-type mammals (Shibata et al. 2013), indicating that extra cartilage formation at the posterior end of the *Ift88* mutant mandible is derived from the enlarged lingual mandibular bone. The enlarged lingual mandibular bone in *Ift88*$^{fl/fl}$*;Wnt1Cre* mice was thus programmed as another mandibular bone. In addition, there was a gap between lingual and buccal mandibular bone formation in the mutant, and Meckel's cartilage was present in the gap. *Ift88*$^{fl/fl}$*;Wnt1Cre* mice thus exhibited mirror-image mandibles between the lingual and buccal

sides of the mandible. These indicate the possibility that mandibular bone formation was duplicated in *Ift88*$^{fl/fl}$*;Wnt1Cre* mice. However, lingual mandibular bone separated from buccal mandibular bone could not be detected on the oral side or the anterior part of the mandible from *Ift88*$^{fl/fl}$*;Wnt1Cre* mice. The duplication of mandibular bone is likely partially to have occurred in *Ift88*$^{fl/fl}$*;Wnt1Cre* mice.

The lack of Hh signaling was observed in most of the mesenchyme from the anterior to the posterior region of *Ift88* mutant mandible. *Smo*$^{fl/fl}$*;Wnt1Cre* mice also showed similar mandibular phenotypes, including two mandibular formations and extra cartilage at the posterior end of the mandibles (Xu et al. 2019). Mirror-image mandibles were also observed in *Smo*$^{fl/fl}$*;Wnt1Cre* mice. These results indicate that mandibular duplication was caused by downregulated Hh signaling. Shh signaling has recently been shown to regulate the patterning of mandibular development (Xu et al. 2019). Shh signaling is activated within primary cilia, and the primary cilia are known to regulate axis patterning (Bisgrove & Yost, 2006; Bimonte et al. 2011; Zaghloul & Brugmann, 2011). It is conceivable that duplication of mandibular bone in *Ift88*$^{fl/fl}$*;Wnt1Cre* mice was caused by abnormal patterning through perturbation of primary cilia function due to *Ift88* deletion and subsequent reduced Shh signaling. The primary cilia thus likely regulate the direction of mandibular bone formation through Hh signaling. On the other hand, deficiency of *Ift88* in osteoblasts and osteocytes has been shown to result in increased bone formation (Yuan & Yang, 2016). The deletion of another ciliary protein, *Kif3a*, has also been reported to lead to ectopic bone formation in the craniobase (Koyama et al. 2007). In addition to abnormal patterning, it is also possible that increased bone formation by perturbation of primary cilia function contributes to enlarged lingual mandibular bone formation in *Ift88*$^{fl/fl}$*;Wnt1Cre* mice. The primary cilia might play a role in limiting bone formation in mesenchyme lingual to Meckel's cartilage in wild-type mandible. Extra bone formation is also observed in maxillary processes of *Ift88*$^{fl/fl}$*;Wnt1Cre* mice, indicating the possibility that limiting bone formation by the primary cilia takes place in many regions during craniofacial development (Watanabe et al. 2019). However, in *Ift88*$^{fl/fl}$*;Wnt1Cre;p53*$^{-/-}$ mice, abnormal bone formation disappears in maxillary processes, but not in mandibles (Watanabe et al. 2019). Molecular mechanisms controlling bone formation by the primary cilia are thus likely to be different between regions.

Hh signaling was downregulated in most of the mandibular mesenchyme of *Ift88*$^{fl/fl}$*;Wnt1Cre* mice. However, the anterior mandibular bone was present and slightly enlarged in *Ift88*$^{fl/fl}$*;Wnt1Cre* mice, although the anterior mandibular bone was absent in *Smo*$^{fl/fl}$*;Wnt1Cre* mice. In addition, the coronoid process was observed in *Smo*$^{fl/fl}$*;Wnt1Cre* mice but not in *Ift88*$^{fl/fl}$*;Wnt1Cre* mice. Thus, the lack of Hh signaling is likely to result in only abnormal lingual mandibular bone formation. Other phenotypes observed in *Ift88*$^{fl/fl}$*;Wnt1Cre* mice including the lack of the coronoid process and the presence and enlargement of the anterior mandibular bone were independent of the lack of Hh signaling. Furthermore, the mandible in *Smo*$^{fl/fl}$*;Wnt1Cre* mice was much smaller than those in *Ift88*$^{fl/fl}$*;Wnt1Cre* mice. The phenotypes of Meckel's cartilage were significantly different between *Ift88*$^{fl/fl}$*;Wnt1Cre* and *Smo*$^{fl/fl}$*;Wnt1Cre* mice. Thus, other molecular changes should have occurred in *Ift88*$^{fl/fl}$*;Wnt1Cre* mice, probably resulting in different phenotypes in *Ift88*$^{fl/fl}$*;Wnt1Cre* mice.

Hh signaling was upregulated in the mandibular epithelium in *Ift88*$^{fl/fl}$*;Wnt1Cre* mice, which was also observed in *Smo*$^{fl/fl}$*;Wnt1Cre* mice. These results suggest that Hh activity in the epithelium is determined by Hh signaling in the mandibular mesenchyme. It is possible that overactivation of Hh signaling in epithelium leads to abnormal mandibular bone formation, since it has been shown that mice with overexpression of Shh in the epithelium (*K14-Shh*) exhibit enlarged mandibles (Cobourne et al. 2009). However, we found no extra mandibular bone formation or abnormal Meckel's cartilage in *R26SmoM2;K14Cre* mice, suggesting that the upregulation of Hh signaling in mandibular epithelium was not the cause of enlarged mandibles in *Ift88*$^{fl/fl}$*;Wnt1Cre* mice. Hh signaling in *R26SmoM2;K14Cre* mice should only be overactivated in the epithelium. However, in *K14-Shh* mice, it is highly likely that overactivation of Shh protein (the Hh ligand) from epithelium can bind to receptors expressed in both epithelium and mesenchyme. It is possible that enlarged mandibles are caused by upregulation of Shh signaling in both the epithelium and mandibular mesenchyme in *K14-Shh* mice.

Acknowledgements

This research was funded by the Japan Society for the Promotion of Science (JSPS; 18K09762).

Conflict of interest

The authors declare that they have no conflict of interest.

References

Achilleos A, Trainor PA (2015) Mouse models of rare craniofacial disorders. *Curr Top Dev Biol* **115**, 413–458.

Adel Al-Lami H, Barrell WB, Liu KJ (2016) Micrognathia in mouse models of ciliopathies. *Biochem Soc Trans* **44**, 1753–1759.

Billmyre KK, Klingensmith J (2015) Sonic hedgehog from pharyngeal arch 1 epithelium is necessary for early mandibular arch cell survival and later cartilage condensation differentiation. *Dev Dyn* **244**, 564–576.

Bimonte S, De Angelis A, Quagliata L, et al. (2011) Ofd1 is required in limb bud patterning and endochondral bone development. *Dev Biol* **349**, 179–191.

Bisgrove BW, Yost HJ (2006) The roles of cilia in developmental disorders and disease. *Development* **133**, 4131–4143.

Brugmann SA, Goodnough LH, Gregorieff A, et al. (2007) Wnt signaling mediates regional specification in the vertebrate face. *Development* **134**, 3283–3295.

Brugmann SA, Allen NC, James AW, et al. (2010) A primary ciliia-dependent etiology for midline facial disorders. *Hum Mol Genet* **19**, 1577–1592.

Cela P, Hampl M, Shylo NA, et al. (2018) Ciliopathy protein Tmem107 plays multiple roles in craniofacial development. *J Dent Res* **97**, 108–117.

Cobourne MT, Xavier GM, Depew M, et al. (2009) Sonic hedgehog signalling inhibits palatogenesis and arrests tooth development in a mouse model of the nevoid basal cell carcinoma syndrome. *Dev Biol* **331**, 38–49.

Danielian PS, Muccino D, Rowitch DH, et al. (1998) Modification of gene activity in mouse embryos *in utero* by a tamoxifen-inducible form of Cre recombinase. *Curr Biol* **8**, 1323–1326.

Gray RS, Abitua PB, Wlodarczyk BJ, et al. (2009) The planar cell polarity effector Fuz is essential for targeted membrane trafficking, ciliogenesis and mouse embryonic development. *Nat Cell Biol* **11**, 1225–1232.

Haycraft CJ, Zhang Q, Song B, et al. (2007) Intraflagellar transport is essential for endochondral bone formation. *Development* **134**, 307–316.

Jeong J, Mao J, Tenzen T, et al. (2004) Hedgehog signaling in the neural crest cells regulates the patterning and growth of facial primordia. *Genes Dev* **18**, 937–951.

Kawasaki M, Porntaveetus T, Kawasaki K, et al. (2014) R-spondins/Lgrs expression in tooth development. *Dev Dyn* **243**, 844–851.

Kitami M, Yamaguchi H, Ebina M, et al. (2019) IFT20 is required for the maintenance of cartilaginous matrix in condylar cartilage. *Biochem Biophys Res Commun* **509**, 222–226.

Kolpakova-Hart E, Jinnin M, Hou B, et al. (2007) Kinesin-2 controls development and patterning of the vertebrate skeleton by Hedgehog- and Gli3-dependent mechanisms. *Dev Biol* **309**, 273–284.

Komatsu Y, Yu PB, Kamiya N, et al. (2013) Augmentation of Smad-dependent BMP signaling in neural crest cells causes craniosynostosis in mice. *J Bone Miner Res* **28**, 1422–1433.

Koyama E, Young B, Nagayama M, et al. (2007) Conditional Kif3a ablation causes abnormal hedgehog signaling topography, growth plate dysfunction, and excessive bone and cartilage formation during mouse skeletogenesis. *Development* **134**, 2159–2169.

Kurosaka H, Iulianella A, Williams T, et al. (2014) Disrupting hedgehog and WNT signaling interactions promotes cleft lip pathogenesis. *J Clin Invest* **124**, 1660–1671.

Li F, Fu G, Liu Y, et al. (2017) ISLET1-dependent β-Catenin/hedgehog signaling is required for outgrowth of the lower jaw. *Mol Cell Biol* **31**, pii: e00590–16.

Mina M, Havens B, Velonis DA (2007) FGF signaling in mandibular skeletogenesis. *Orthod Craniofac Res* **10**, 59–66.

Murcia NS, Richards WG, Yoder BK, et al. (2000) The Oak Ridge Polycystic Kidney (orpk) disease gene is required for left-right axis determination. *Development* **127**, 2347–2355.

Narai S, Kodama Y, Maeda Y, et al. (2006) Trp53 affects the developmental anomaly of clefts of the palate in irradiated mouse embryos but not clefts of the lip with or without the palate. *Radiat Res* **166**, 877–882.

Ohazama A, Johnson EB, Ota MS, et al. (2008) Lrp4 modulates extracellular integration of cell signaling pathways in development. *PLoS ONE* **3**, e4092.

Oka K, Oka S, Hosokawa R, et al. (2008) TGF-beta mediated Dlx5 signaling plays a crucial role in osteo-chondroprogenitor cell lineage determination during mandible development. *Dev Biol* **321**, 303–309.

Parada C, Chai Y (2015) Mandible and tongue development. *Curr Top Dev Biol* **115**, 31–58.

Shibata S, Sato R, Murakami G, et al. (2013) Origin of mandibular condylar cartilage in mice, rats, and humans: periosteum or separate blastema? *J Oral Biosci* **55**, 208–216.

Terrazas K, Dixon J, Trainor PA, et al. (2017) Rare syndromes of the head and face: mandibulofacial and acrofacial dysostoses. *Wiley Interdiscip Rev Dev Biol* **6**, e263. https://doi.org/10.1002/wdev.263

Tian H, Feng J, Li J, et al. (2017) Intraflagellar transport 88 (IFT88) is crucial for craniofacial development in mice and is a candidate gene for human cleft lip and palate. *Hum Mol Genet* **26**, 860–872.

Watanabe M, Kawasaki M, Kawasaki K, et al. (2019) Ift88 limits bone formation in maxillary process through suppressing apoptosis. *Arch Oral Biol* **27, 101**, 43–50.

Xu J, Liu H, Lan Y, et al. (2019) Hedgehog signaling patterns the oral-aboral axis of the mandibular arch. *Elife* **8**, e40315. https://doi.org/10.7554/eLife.40315

Yi R, O'Carroll D, Pasolli HA, et al. (2006) Morphogenesis in skin is governed by discrete sets of differentially expressed microRNAs. *Nat Genet* **38**, 356–362.

Yuan X, Yang S (2016) Primary cilia and intraflagellar transport proteins in bone and cartilage. *J Dent Res* **95**, 1341–1349.

Zaghloul NA, Brugmann SA (2011) The emerging face of primary cilia. *Genesis* **49**, 231–246.

Zhang Z, Wlodarczyk BJ, Niederreither K, et al. (2011) Fuz regulates craniofacial development through tissue specific responses to signaling factors. *PLoS ONE* **6**, e24608.

Supporting Information

Additional Supporting Information may be found in the online version of this article:

Fig. S1. Mandibular bone phenotypes in *Ift88$^{fl/fl}$;Wnt1Cre*. Aboral (A,B) and oral (C–F) view of skeletal preparation of wild-type and *Ift88$^{fl/fl}$;Wnt1Cre* in the posterior (A–D) and anterior (E,F) region at E18.5. Scale bars: 1 mm.

Fig. S2. Initiation of extra mandibular bone formation. (A,B) Frontal sections showing the developing mandible at E13.5. Arrows indicating ectopic condensed mesenchyme. (C,D) Frontal sections showing BrdU-positive cells in wild-type and *Ift88$^{fl/fl}$;Wnt1Cre* mice at E12.5. Arrows indicating region corresponding ectopic bone. Meckel's cartilage was outlined by blue dots. Scale bars: 500 μm.

Fig. S3. Overactivation of Hh signaling in epithelium in mandibular development. Frontal sections showing the developing mandibular bone in wild-type and *R26SmoM2$^{fl/fl}$;K14Cre* mice. Scale bars: 500 μm.

Fig. S4. Mandibular bone phenotype in *Ift88$^{fl/fl}$;Wnt1Cre;p53$^{-/-}$*. Frontal sections showing the developing mandibular bone in *Ift88$^{fl/fl}$;Wnt1Cre* (A) and *Ift88$^{fl/fl}$;Wnt1Cre;p53$^{-/-}$* (B,C) mice at E18.5. Scale bars: 500 μm.